

Glycolysis in Bloodstream Form *Trypanosoma brucei* Can Be Understood in Terms of the Kinetics of the Glycolytic Enzymes*

(Received for publication, July 10, 1996, and in revised form, October 9, 1996)

Barbara M. Bakker^{‡§}, Paul A. M. Michels[¶], Fred R. Opperdoes[¶], and Hans V. Westerhoff^{‡||}

From the [‡]Microbial Physiology, BioCentrum Amsterdam, Vrije Universiteit, De Boelelaan 1087, NL-1081 HV Amsterdam, [§]E. C. Slater Institute, BioCentrum Amsterdam, University of Amsterdam, Plantage Muidergracht 12, NL-1018 TV Amsterdam, The Netherlands, and the [¶]Research Unit for Tropical Diseases, International Institute of Cellular and Molecular Pathology and Laboratory of Biochemistry, Catholic University of Louvain, Avenue Hippocrate 74, B-1200 Brussels, Belgium

In trypanosomes the first part of glycolysis takes place in specialized microbodies, the glycosomes. Most glycolytic enzymes of *Trypanosoma brucei* have been purified and characterized kinetically. In this paper a mathematical model of glycolysis in the bloodstream form of this organism is developed on the basis of all available kinetic data. The fluxes and the cytosolic metabolite concentrations as predicted by the model were in accordance with available data as measured in non-growing trypanosomes, both under aerobic and under anaerobic conditions. The model also reproduced the inhibition of anaerobic glycolysis by glycerol, although the amount of glycerol needed to inhibit glycolysis completely was lower than experimentally determined. At low extracellular glucose concentrations the intracellular glucose concentration remained very low, and only at 5 mM of extracellular glucose, free glucose started to accumulate intracellularly, in close agreement with experimental observations. This biphasic relation could be related to the large difference between the affinities of the glucose transporter and hexokinase for intracellular glucose. The calculated intraglycosomal metabolite concentrations demonstrated that enzymes that have been shown to be near-equilibrium in the cytosol must work far from equilibrium in the glycosome in order to maintain the high glycolytic flux in the latter.

NADH produced in the glycosomes by glyceraldehyde-3-phosphate dehydrogenase (GAPDH) is used to reduce dihydroxyacetone phosphate (DHAP) to glycerol 3-phosphate (Gly-3-P). Subsequently, Gly-3-P is reoxidized by molecular oxygen via a glycerol-3-phosphate oxidase (GPO) in the mitochondria, and DHAP returns to the glycosomes. In the organelles there is no net ATP production or consumption by glycolysis, since the consumption of ATP by hexokinase (HK) and phosphofructokinase (PFK) is balanced by phosphoglycerate kinase (PGK). Only in the cytosol there is net glycolytic ATP production by pyruvate kinase (PYK). Under anaerobic conditions Gly-3-P is converted to glycerol with the concomitant production of ATP via the reverse action of glycerol kinase (GK) (1, 2, 6, 7). Unlike the corresponding enzymes in most other organisms, the glycosomal HK and PFK of trypanosomes are hardly subject to allosteric regulation (8–10). In trypanosomes not PFK but PYK is activated by fructose 2,6-bisphosphate (11–13), and consistently, 6-phosphofructo-2-kinase and fructose-2,6-bisphosphatase are found in the cytosol (14).

Trypanosoma brucei, the parasite that causes African sleeping disease in humans and nagana in livestock, is transmitted by the tse-tse fly. When living in the mammalian bloodstream *T. brucei* has neither a functional Krebs cycle nor oxidative phosphorylation nor does it store any carbohydrates. Consequently, complete inhibition of glycolysis kills the organism. Because of the differences between mammalian and trypanosomal glycolysis, this pathway is a major potential target for drugs against the African sleeping disease (15). Many of the glycolytic enzymes of trypanosomes resemble, however, the corresponding enzymes of the hosts of the latter. A drug that interferes strongly with trypanosome glycolysis may well compromise this metabolic pathway in its host where glycolysis is also essential. Consequently, it is important to design drugs that strongly inhibit glycolysis in trypanosomes but only weakly that of their hosts. This design task is complicated by the fact that the effect of modulation of an enzyme activity on a metabolic flux also depends on the properties of other enzymes in the metabolic pathway (16–18). Nevertheless, recent developments may well bring such rational drug design within reach. In the past decade most glycolytic enzymes of *T. brucei* have been purified and characterized extensively, both structurally and kinetically. Furthermore, fluxes and glycolytic in-

In several respects glycolysis in trypanosomes differs from glycolysis in other eukaryotes. In these parasites most glycolytic enzymes occur sequestered in a specialized organelle closely related to peroxisomes (1) (for reviews see Refs. 2–5). As in trypanosomes 90% of the protein content of these microbodies consists of glycolytic enzymes; they are called glycosomes. In glycosomes glucose is converted to 3-phosphoglycerate (3-PGA),¹ which is metabolized to pyruvate in the cytosol. The

* This study was supported by the Netherlands Organization for Scientific Research (NWO) and the Netherlands Association of Biotechnology Research Schools (ABON). The costs of publication of this article were defrayed in part by the payment of page charges. This article must therefore be hereby marked "advertisement" in accordance with 18 U.S.C. Section 1734 solely to indicate this fact.

|| To whom correspondence should be addressed: Microbial Physiology, BioCentrum Amsterdam, Vrije Universiteit, De Boelelaan 1087, NL-1081 HV Amsterdam, The Netherlands. Tel.: +31 20 4447228; Fax: +31 20 4447229; E-mail: hw@bio.vu.nl.

¹ The abbreviations used are: 3-PGA, 3-phosphoglycerate; AK, adenylate kinase; ALD, fructose-1,6-bisphosphate aldolase; 1,3-BPGA, 1,3-bisphosphoglycerate; DHAP, dihydroxyacetone phosphate; ENO, enolase; Fru-1,6-BP, fructose 1,6-bisphosphate; Fru-6-P, fructose 6-phosphate; Glc, glucose; Γ , ratio of product and substrate concentrations; GA-3-P, glyceraldehyde 3-phosphate; GAPDH, glyceraldehyde-3-phosphate dehydrogenase; GDH, glycerol-3-phosphate dehydrogenase;

GK, glycerol kinase; Gly-3-P, glycerol 3-phosphate; Glc-6-P, glucose 6-phosphate; GPO, glycerol-3-phosphate oxidase; HK, hexokinase; [Glc]_i, intracellular glucose; K_{eq} , equilibrium constant; k_{cat} , turnover rate; K_M , Michaelis constant; [Glc]_o, extracellular glucose; PEP, phosphoenolpyruvate; 2-PGA, 2-phosphoglycerate; PGI, glucose-phosphate isomerase; PFK, phosphofructokinase; PGK, phosphoglycerate kinase; PGM, phosphoglycerate mutase; PYK, pyruvate kinase; TIM, triosephosphate isomerase.

intermediates have been measured under various conditions. Although the individual enzyme kinetic data are available, their implications for the glycolytic pathway as a whole have not been evaluated nor has it been attempted to predict the effect on glycolysis even for a drug for which the effects on its target enzyme are known.

In this paper we relate the functioning of glycolysis in bloodstream form *T. brucei* to the known kinetics of the individual trypanosome enzymes. To this end a detailed computer model of trypanosomal glycolysis has been constructed, including all available enzyme kinetics. The model distinguishes itself from other elaborate kinetic glycolysis models in the sense that the kinetic parameters are not adjusted to fit the measured metabolite concentrations (19–21). *T. brucei* is a very suitable organism for this type of modeling because its glycolysis lacks many branches (*cf.* in other organisms (22)), the glycosomal enzymes lack allosteric regulation, and because most trypanosomal enzymes have been characterized under the same experimental conditions. The model predicts how the steady-state glycolytic flux and metabolite concentrations depend on the substrate and product concentrations and the enzyme-kinetic parameters in non-growing cells. It explains certain aspects of cell physiology, but it also makes us aware which data are still lacking for a deeper understanding.

MATERIALS AND METHODS

This section describes how the model was constructed and what equations were used.

Stoichiometry and Conserved Moieties—The model contains the glycolytic pathway, including the branch to glycerol and the utilization of ATP (Fig. 1). The two glucose transport steps, *i.e.* across the plasma membrane and the glycosomal membrane, were lumped into one, because in kinetic experiments no distinction between them has been made so far (23). The glycosomal membrane was taken to be impermeable to metabolites (24), except for those that need to be transported across this membrane (Fig. 1). Nothing is known about the kinetics of the transport of 3-PGA, Gly-3-P, and DHAP. These steps were assumed to be in equilibrium and mutually independent. The concentration of inorganic phosphate in the glycosome was assumed to be saturating. At steady state adenylate kinase (AK) should be at equilibrium. When the known kinetics of glucose-phosphate isomerase (PGI) (25) and triose-phosphate isomerase (TIM) (26) were implemented explicitly, these enzymes operated close to equilibrium (the ratio of the steady-state product and substrate concentrations divided by the equilibrium constant exceeded 0.8 for both reactions), and therefore, they were further treated as equilibrium reactions. This facilitated the calculations with hardly any effect on the outcome. Experimentally it has been shown that the cytosolic enzymes phosphoglycerate mutase (PGM) and enolase (ENO) operate near equilibrium (27). Accordingly, they were treated as if in equilibrium. Finally, the transport of glycerol out of the cells was assumed to be in equilibrium. The kinetics of all other enzymes and the transport of glucose and pyruvate were implemented explicitly in the model.

Four moiety conservation relations were derived from the stoichiometry as depicted in Fig. 1 by using the metabolic modeling program SCAMP (28). These correspond to the adenine nucleotides in the glycosome and the cytosol, respectively, the nicotinamide adenine nucleotides in the glycosome, and the organic phosphate that is not exchanged with inorganic phosphate. None of the reactions modifies these sums:

$$[\text{ATP}]_g + [\text{ADP}]_g + [\text{AMP}]_g = C_1 \quad (\text{Eq. 1})$$

$$[\text{ATP}]_c + [\text{ADP}]_c + [\text{AMP}]_c = C_2 \quad (\text{Eq. 2})$$

$$[\text{NADH}]_g + [\text{NAD}]_g = C_3 \quad (\text{Eq. 3})$$

$$[\text{Gly-3-P}]_g V_g + [\text{Gly-3-P}]_c V_c + [\text{DHAP}]_g V_g + [\text{DHAP}]_c V_c + [\text{Glc-6-P}]_g V_g + [\text{Fru-6-P}]_g V_g + 2[\text{Fru-1,6-BP}]_g V_g + [\text{GA-3-P}]_g V_g + [1,3\text{-BPGA}]_g V_g + 2[\text{ATP}]_g V_g + [\text{ADP}]_g V_g = C_4 \cdot V_g \quad (\text{Eq. 4})$$

The $[\]_c$ refers to the cytosolic concentration and the $[\]_g$ to the glycosomal concentration. V_c is the cytosolic volume and V_g the glycosomal volume in μl per mg of cell protein. In Equation 4 the concentrations of

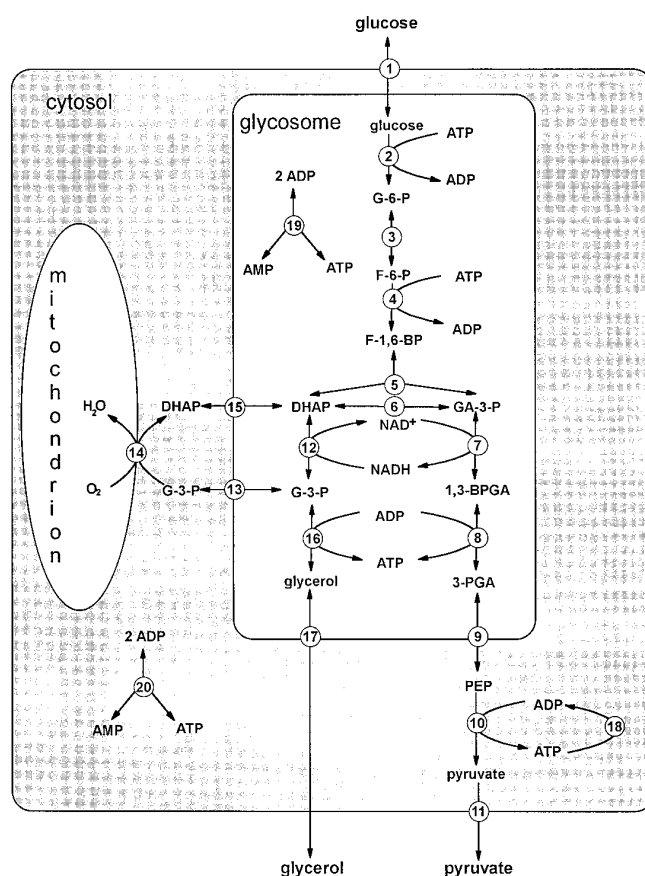


FIG. 1. The stoichiometric scheme of the model of glycolysis in bloodstream form *T. brucei*. The reactions 3, 6, 9, 13, 15 and 17, 19 and 20 were treated as equilibrium reactions. 1, transport of glucose across the plasma membrane and the glycosomal membrane; 2, HK; 3, PGI; 4, PFK; 5, ALD; 6, TIM; 7, GAPDH; 8, PGK; 9, transport of 3-PGA across the glycosomal membrane, PGM, and ENO; 10, PYK; 11, pyruvate transport across the plasma membrane; 12, GDH; 13, transport of Gly-3-P (G-3-P) across the glycosomal membrane; 14, GPO; 15, transport of DHAP across the glycosomal membrane; 16, GK; 17, transport of glycerol across the glycosomal membrane and the plasma membrane; 18, ATP utilization; 19, glycosomal AK; 20, cytosolic AK. G-6-P, Glc-6-P; F-6-P, Fru-6-P; F-1, 6-BP, Fru-1, 6-BP.

Fru-1,6-BP and ATP are multiplied by a factor of 2, because these metabolites contain two phosphate groups that are transferred to other organic compounds. As Gly-3-P and DHAP were assumed to equilibrate across the glycosomal membrane, Equation 4 simplified to

$$([\text{Gly-3-P}] + [\text{DHAP}]) \left(1 + \frac{V_c}{V_g}\right) + [\text{Glc-6-P}]_g + [\text{Fru-6-P}]_g + 2[\text{Fru-1,6-BP}]_g + [\text{GA-3-P}]_g + [1,3\text{-BPGA}]_g + 2[\text{ATP}]_g + [\text{ADP}]_g = C_4 \quad (\text{Eq. 5})$$

in which

$$[\text{Gly-3-P}] \equiv [\text{Gly-3-P}]_g = [\text{Gly-3-P}]_c \quad (\text{Eq. 6})$$

and

$$[\text{DHAP}] \equiv [\text{DHAP}]_g = [\text{DHAP}]_c \quad (\text{Eq. 7})$$

The two distinct pools of adenine nucleotides occur as a consequence of the assumed impermeability of the glycosomal membrane for these compounds. The fourth conserved moiety (Equations 4 and 5) is also a consequence of the compartmentation. If glycolysis occurred in one compartment, ATP utilization (Reaction 18 in Fig. 1), for example, would modify this sum. As the glycosomes occupy 4.3% of the total cellular volume (29), the ratio V_c/V_g amounts to 22.3. C_2 and C_4 were estimated from Ref. 27, by using that 1 g wet weight corresponds to 80 mg of protein and 1 ml of total cellular volume corresponds to 175 mg of

TABLE I
The V_{\max} values in the catabolic direction (V^+) for all enzymes included in the model

The V_{\max} values of the glycosomal enzymes were derived from the reported glycosomal enzyme concentrations and from the turnover rates (k_{cat}) reported after *in vitro* measurements. Other V_{\max} values were based on reported transport and activity assays. The V_{\max} of pyruvate transport was estimated as described in the text.

Enzyme	Concentration (% of cell protein) (46)	k_{cat} ($\mu\text{mol min}^{-1}$ (mg enzyme) $^{-1}$)	V_{\max} (nmol min $^{-1}$ (mg cell protein) $^{-1}$)
Glucose transport			106.2 (23)
HK	0.25	250 ^a	625
PFK	0.39	200 (10)	780
ALD	1.23	15 (35)	184.5
GAPDH	0.50	294 (48)	1470
PGK	0.16	400 (49)	640
PYK			2.6·10 ³ (7)
GDH	0.25	170 ^b	425
GPO			368 or 0 ^{c,d} (50)
GK			0 or 200 ^c
Pyruvate transport			160

^a A.-M. Loiseau, unpublished results.

^b M. Callens, D. Kuntz, O. Bos, and F. Opperdoes, unpublished results.

^c To simulate aerobic conditions GK was switched off ($V_{\max} = 0$) and to simulate anaerobic conditions GPO was switched off (see "Substrate and Product Concentrations").

^d The V_{\max} of GPO was expressed as nmol Gly-3-P min $^{-1}$ (mg cell protein) $^{-1}$. Two molecules of Gly-3-P are converted per molecule of O₂.

total cell protein (29). C_1 and C_3 were chosen arbitrarily, but their values hardly affected the results. The values were $C_1 = 3.9$ mM, $C_2 = 3.9$ mM, $C_3 = 4$ mM, and $C_4 = 120$ mM. This value for C_4 is just saturating; an increase does not affect the flux. C_4 is high, because [Gly-3-P] and [DHAP] are multiplied by the factor $1 + V_c/V_g$. Only when [Gly-3-P] and [DHAP] become low, this high sum implies high concentrations of the glycosomal metabolites. This did not occur in the simulations reported in this paper (results not shown).

Kinetic Equations—All available literature data (Tables I and II) on trypanosome enzyme kinetics have been obtained at 25 °C, except for glucose transport (37 °C) (23).

The kinetics of GPO and the transport of pyruvate across the plasma membrane were described by irreversible Michaelis-Menten kinetics:

$$v = V^+ \cdot \frac{S}{1 + \frac{S}{K_S}} \quad (\text{Eq. 8})$$

in which S is the substrate concentration. The measured rate of zero-*trans* pyruvate influx was well below the steady-state rate of pyruvate production (30). This may be due to asymmetry of the transporter, but most probably the long time scale of the uptake assay (30 s) (30) also led to an underestimation of the rate, because pyruvate cannot be metabolized and accumulates. Therefore the V_{\max} for efflux was adjusted so that the pyruvate concentration in the model agreed with the measured intracellular pyruvate concentration of 21 mM (31).

The kinetics of HK were described by a Michaelis-Menten type equation for two substrates:

$$v = V^+ \cdot \frac{\frac{S_1}{K_{S1}} \cdot \frac{S_2}{K_{S2}}}{\left(1 + \frac{S_1}{K_{S1}} + \frac{P_1}{K_{P1}}\right) \cdot \left(1 + \frac{S_2}{K_{S2}}\right)} \quad (\text{Eq. 9})$$

in which S_1 is ATP, S_2 is intracellular glucose, and P_1 is ADP. Thus the competitive product inhibition by ADP was included. Glucose 6-phosphate (Glc-6-P) had no effect on the rate (8).

The kinetics of GAPDH, PGK, glycerol-3-phosphate dehydrogenase (GDH), and GK were described by a reversible Michaelis-Menten equation for two non-competing product-substrate couples:

$$v = V^+ \cdot \frac{\frac{S_1}{K_{S1}} \cdot \frac{S_2}{K_{S2}} \cdot \frac{V^-}{V^+} \cdot \frac{P_1}{K_{P1}} \cdot \frac{P_2}{K_{P2}}}{\left(1 + \frac{S_1}{K_{S1}} + \frac{P_1}{K_{P1}}\right) \cdot \left(1 + \frac{S_2}{K_{S2}} + \frac{P_2}{K_{P2}}\right)} \quad (\text{Eq. 10})$$

The transport of glucose was described according to a 4-state model for a facilitated diffusion carrier (32). The experimental data (33) may indicate that the carrier is slightly asymmetric. However, the V_{\max} measured for efflux is lower than that for influx, whereas the K_M for efflux is higher. As this would lead to a net flux in the absence of a

glucose gradient, the apparent asymmetry was neglected. Rewritten into a Michaelis-Menten-like form the equations became:

$$v_{\text{glucose transport}} = V^+ \frac{[\text{Glc}]_o - [\text{Glc}]_i}{K_{\text{Glc}} + [\text{Glc}]_o + [\text{Glc}]_i + \alpha \cdot [\text{Glc}]_o \cdot [\text{Glc}]_i / K_{\text{Glc}}} \quad (\text{Eq. 11})$$

in which $[\text{Glc}]_o$ and $[\text{Glc}]_i$ are the extracellular and intracellular glucose concentrations, respectively, and K_{Glc} is 2 mM (23). From the assumed symmetry of the carrier and from the finding that the V_{\max} for equilibrium exchange was twice as high as the V_{\max} for zero *trans*-influx, the factor α was calculated to be 0.75.

The rate of PFK exhibits a slightly cooperative dependence on the concentration of fructose 6-phosphate (Fru-6-P):

$$v_{\text{PFK}} = V^+ \cdot \frac{\left(\frac{[\text{Fru-6-P}]}{K_{M,\text{Fru6P}}}\right)^n \cdot \left(\frac{[\text{ATP}]}{K_{M,\text{ATP}}}\right)}{\left(1 + \left(\frac{[\text{Fru-6-P}]}{K_{M,\text{Fru6P}}}\right)^n\right) \cdot \left(1 + \frac{[\text{ATP}]}{K_{M,\text{ATP}}}\right)} \quad (\text{Eq. 12})$$

in which $K_{M,\text{Fru6P}} = 0.82$ mM, $K_{M,\text{ATP}} = 2.6 \cdot 10^{-2}$ mM, and $n = 1.2$ (9, 10).

The rate of PYK depends cooperatively on the concentration of PEP:

$$v_{\text{PYK}} = V^+ \cdot \frac{\left(\frac{[\text{PEP}]}{K_{M,\text{PEP}}}\right)^n \cdot \left(\frac{[\text{ADP}]}{K_{M,\text{ADP}}}\right)}{\left(1 + \left(\frac{[\text{PEP}]}{K_{M,\text{PEP}}}\right)^n\right) \cdot \left(1 + \frac{[\text{ADP}]}{K_{M,\text{ADP}}}\right)} \quad (\text{Eq. 13})$$

in which $K_{M,\text{PEP}} = 0.34 \cdot (1 + [\text{ATP}]_o / 0.57 \text{ mM} + [\text{ADP}]_o / 0.64 \text{ mM})$ mM, $K_{M,\text{ADP}} = 0.114$ mM and $n = 2.5$ (12, 13). The equation for $K_{M,\text{PEP}}$ was fitted to the measurements of this parameter at different concentrations of ATP and ADP (12). Variable activation of PYK by fructose 2,6-bisphosphate (12) was neglected, as the concentration of this compound was largely saturating in bloodstream form trypanosomes in the presence of glucose (14), and consequently it is unlikely that it plays a regulatory role under these conditions.

Aldolase (ALD) works according to an ordered uni-bi mechanism. Glycerinaldehyde 3-phosphate (GA-3-P) dissociates from the enzyme before DHAP does (34, 35). The rate equation reads:

$$v_{\text{ALD}} = V^+ \cdot \frac{\frac{[\text{Fru-1,6-BP}]}{K_{M,\text{F16BP}}} \cdot \frac{V^- [\text{GA-3-P}][\text{DHAP}]}{K_{M,\text{GA3P}} K_{M,\text{DHAP}}}}{\left(1 + \frac{[\text{Fru-1,6-BP}]}{K_{M,\text{F16BP}}} + \frac{[\text{GA-3-P}]}{K_{M,\text{GA3P}}} + \frac{[\text{DHAP}]}{K_{M,\text{DHAP}}}\right) \cdot \left(\frac{[\text{Fru-1,6-BP}][\text{GA-3-P}]}{K_{M,\text{F16BP}} K_{i,\text{GA3P}}} + \frac{[\text{GA-3-P}][\text{DHAP}]}{K_{M,\text{GA3P}} K_{M,\text{DHAP}}}\right)} \quad (\text{Eq. 14})$$

in which $V^-/V^+ = 1.19$, $K_{M,\text{F16BP}} = 9 \cdot 10^{-3}$ (1 + $[\text{ATP}]_o / 0.68$ mM + $[\text{ADP}]_o / 1.51$ mM + $[\text{AMP}]_o / 3.65$ mM) mM, $K_{M,\text{GA3P}} = 6.7 \cdot 10^{-2}$ mM, $K_{M,\text{DHAP}} = 1.5 \cdot 10^{-2}$ mM, and $K_{i,\text{GA3P}} = 9.8 \cdot 10^{-2}$ mM (35).

TABLE II
Kinetic parameters of the enzymes described by Michaelis-Menten-type kinetics

One-substrate reactions		Two-substrate reactions					
Enzyme	K_S	Enzyme	V^-/V^+	K_{S1}	K_{S2}	K_{P1}	K_{P2}
	<i>mM</i>			<i>mM</i>	<i>mM</i>	<i>mM</i>	<i>mM</i>
GPO	1.7 (Gly-3-P) (50)	HK (8)		0.116 (ATP)	0.1 (Glc _c) ^a	0.126 (ADP)	
Pyruvate transport	1.96 (PYR _c) ^d (30)	GAPDH (48)	0.67	0.15 (GA-3-P)	0.45 (NAD ⁺)	0.1 (1,3-BPGA)	0.02 (NADH)
		PGK (49)	0.029 ^b	0.05 (1,3-BPGA) ^b	0.1 (ADP) ^b	1.62 (3-PGA)	0.29 (ATP)
		GDH ^c	0.07	0.85 (DHAP)	0.015 (NADH)	6.4 (Gly-3-P)	0.6 (NAD ⁺)
		GK (6)	167	5.1 (Gly-3-P)	0.12 (ADP)	0.12 (Gly)	0.19 (ATP)

^a A.-M. Loiseau, unpublished results.

^b Conjectured, in agreement with an equilibrium constant of $3.3 \cdot 10^3$ in the catabolic direction (51).

^c M. Callens, D. Kuntz, O. Bos, and F. Opperdoes, unpublished results.

^d c, Cytosolic.

The hydrolysis of ATP for free-energy-dissipating processes, such as motion, biosynthesis, and the maintenance of the proton gradients across the plasma membrane and the mitochondrial membrane (36, 37), cannot be described by a simple and realistic equation based on the mechanism of these processes. Therefore, a phenomenological equation was constructed. Under steady-state conditions the flux through pyruvate kinase should equal ATP hydrolysis. In the absence of ATP the utilization rate should be zero. The ratios under anaerobic and aerobic conditions were 1.2 and 2.9 (27), respectively, and the rate of pyruvate production, and hence ATP utilization, under aerobic conditions was twice the rate under anaerobic conditions (38). As the relation between the rate of ATP utilization and the [ATP]/[ADP] ratio seemed close to linear, we assumed

$$v_{\text{ATP utilization}} = k \cdot \frac{[\text{ATP}]}{[\text{ADP}]} \quad (\text{Eq. 15})$$

This rate equation corresponds to a far-from-equilibrium Michaelis-Menten reaction with dominant product inhibition. The value of k was adjusted to $50 \text{ nmol min}^{-1} \text{ mg protein}^{-1}$, so that the calculated steady-state [ATP]/[ADP] ratio under aerobic conditions corresponded to the measured ratio. Equation 15 should not be extrapolated to very high [ATP]/[ADP] ratios.

Substrate and Product Concentrations—The extracellular concentrations of glucose, O₂, pyruvate, and glycerol were treated as parameters of the system, which means that they were fixed for each steady-state calculation. Glucose was 5 mM, which is the concentration the trypanosomes encounter in the bloodstream (23). O₂ was taken to be saturating under aerobic conditions, whereas the flux through GPO was completely blocked under anaerobic conditions by setting the V_{max} of GPO to zero. In the absence of glycerol, 10% of the total flux went to glycerol under aerobic conditions in contradiction with the corresponding experimental finding that no glycerol was produced (38). However, in the model only 0.5 μM of glycerol was required to inhibit this flux, and at higher concentrations it was reversed. If one were to allow free accumulation of glycerol, the GK reaction should reach equilibrium. The aerobic steady state was identical but easier to compute if the V^+ of GK was set to zero. The extracellular concentration of pyruvate and both the extracellular and the intracellular concentrations of glycerol were zero unless specified otherwise.

Differential Equations—If a reaction in the pathway was considered to be in equilibrium, its products and substrates were treated as a single metabolite pool. To this aim five pools were defined.

The sum of hexose phosphates in the glycosome is

$$[\text{hexose-P}]_g \equiv [\text{Glc-6-P}]_g + [\text{Fru-6-P}]_g \quad (\text{Eq. 16})$$

The sum of triose phosphates is

$$[\text{triose-P}] = \frac{[\text{DHAP}]_c V_c + [\text{DHAP}]_g V_g + [\text{GA-3-P}]_g V_g}{V_{\text{tot}}} \quad (\text{Eq. 17})$$

$$= \frac{[\text{DHAP}] \left(1 + \frac{V_c}{V_g} \right) + [\text{GA-3-P}]_g}{\left(1 + \frac{V_c}{V_g} \right)}$$

A pool [N] was defined by

$$[\text{N}] \equiv \frac{[3\text{-PGA}](V_g + V_c) + [2\text{-PGA}]_c V_c + [\text{PEP}]_c V_c}{V_{\text{tot}}} \quad (\text{Eq. 18})$$

in which

$$[3\text{-PGA}] \equiv [3\text{-PGA}]_c = [3\text{-PGA}]_g \quad (\text{Eq. 19})$$

Consequently,

$$[\text{N}] = \frac{[3\text{-PGA}] \left(1 + \frac{V_c}{V_g} \right) + [2\text{-PGA}]_c \frac{V_c}{V_g} + [\text{PEP}]_c \frac{V_c}{V_g}}{\left(1 + \frac{V_c}{V_g} \right)} \quad (\text{Eq. 20})$$

Finally two variables P_g and P_c , denoting the sums of high energy phosphates in the glycosome and the cytosol, respectively, were defined:

$$P_g \equiv 2[\text{ATP}]_g + [\text{ADP}]_g \quad (\text{Eq. 21})$$

$$P_c \equiv 2[\text{ATP}]_c + [\text{ADP}]_c \quad (\text{Eq. 22})$$

The following set of differential equations described the time-dependent behavior of glycolysis:

$$\frac{d[\text{Glc}]_i}{dt} = \frac{(v_{\text{glucose transport}} - v_{\text{HK}})}{V_{\text{tot}}} \quad (\text{Eq. 23})$$

$$\frac{d[\text{hexose-P}]_g}{dt} = \frac{(v_{\text{HK}} - v_{\text{PFK}})}{V_g} \quad (\text{Eq. 24})$$

$$\frac{d[\text{Fru-1,6-BP}]_g}{dt} = \frac{(v_{\text{PFK}} - v_{\text{ALD}})}{V_g} \quad (\text{Eq. 25})$$

$$\frac{d[\text{triose-P}]}{dt} = \frac{2v_{\text{ALD}} - v_{\text{GAPDH}} - v_{\text{GDH}} + v_{\text{GPO}}}{V_{\text{tot}}} \quad (\text{Eq. 26})$$

$$\frac{d[1,3\text{-BPGA}]_g}{dt} = \frac{(v_{\text{GAPDH}} - v_{\text{PGK}})}{V_g} \quad (\text{Eq. 27})$$

$$\frac{d[\text{N}]}{dt} = \frac{v_{\text{PGK}} - v_{\text{PYK}}}{V_{\text{tot}}} \quad (\text{Eq. 28})$$

$$\frac{d[\text{PYR}]_c}{dt} = \frac{(v_{\text{PYK}} - v_{\text{pyruvate transport}})}{V_c} \quad (\text{Eq. 29})$$

$$\frac{d[\text{NADH}]_g}{dt} = \frac{(v_{\text{GAPDH}} - v_{\text{GDH}})}{V_g} \quad (\text{Eq. 30})$$

$$\frac{dP_g}{dt} = \frac{(-v_{\text{HK}} - v_{\text{PFK}} + v_{\text{PGK}} + v_{\text{GK}})}{V_g} \quad (\text{Eq. 31})$$

$$\frac{dP_c}{dt} = \frac{(v_{\text{PYK}} - v_{\text{ATP utilization}})}{V_c} \quad (\text{Eq. 32})$$

The total intracellular volume V_{tot} was taken constant at $5.7 \mu\text{l/mg}$ total cellular protein (29). The time t was expressed in minutes and the enzyme rates v in $\text{nmol min}^{-1} (\text{mg cell protein})^{-1}$. In order to obtain the time derivatives of the concentrations in mM min^{-1} , a correction was made for the volume of the compartment in which a metabolite pool resides. As the K_M values were expressed in mM, the metabolite concentrations were obtained in mM as well.

To calculate a steady state all above time derivatives of metabolite concentrations were set to zero. The resulting system of nonlinear equations was solved numerically for the metabolite concentrations.

TABLE III
The equilibrium constants at 25 °C of the reactions treated as equilibrium reactions (51)

Enzyme	K_{eq}
PGI	0.29
TIM	0.045
PGM	0.187
ENO	6.7
AK	0.442

The concentrations of NAD^+ and Gly-3-P were calculated from the conservation equations (Equations 3 and 5, respectively). The other dependent concentrations were calculated from the equilibrium conditions as described below.

Equilibrium Reactions—The equilibrium constants are found in Table III. The transport of metabolites across the glycosomal membrane was assumed to be driven only by concentration gradients of these metabolites, and consequently, the corresponding equilibrium constants were 1. The individual metabolite concentrations were calculated from the equilibrium pools as follows.

a, $Glc-6-P_g \leftrightarrow Fru-6-P_g$. The equilibrium equation reads

$$\frac{[Fru-6-P]_g}{[Glc-6-P]_g} = K_{eq,PGI} \quad (\text{Eq. 33})$$

It follows from Equations 16 and 33 that

$$[Glc-6-P]_g = \frac{[\text{hexose} - P]_g}{K_{eq,PGI}} \quad (\text{Eq. 34})$$

When $[Glc-6-P]_g$ was known $[Fru-6-P]_g$ was calculated from Equation 16.

b, $DHAP_c \leftrightarrow DHAP_g \leftrightarrow GA-3-P_g$. The equilibrium equation of TIM is

$$\frac{[GA-3-P]_g}{[DHAP]_g} = K_{eq,TIM} \quad (\text{Eq. 35})$$

It follows from Equations 7, 17, and 35 that

$$[DHAP] = \frac{[\text{triose-P}] \left(1 + \frac{V_c}{V_g}\right)}{1 + \frac{V_c}{V_g} + K_{eq,TIM}} \quad (\text{Eq. 36})$$

When $[DHAP]$ was known $[GA-3-P]_g$ was calculated from Equation 17.

c, $3-PGA_g \leftrightarrow 3-PGA_c \leftrightarrow 2-PGA_c \leftrightarrow PEP_c$

The equilibrium equations of PGM and ENO are

$$\frac{[2-PGA]_c}{[3-PGA]_c} = K_{eq,PGM} \quad (\text{Eq. 37})$$

$$\frac{[PEP]_c}{[2-PGA]_c} = K_{eq,ENO} \quad (\text{Eq. 38})$$

From Equations 19, 20, 37, and 38 it follows that

$$[3-PGA] = \frac{[N] \left(1 + \frac{V_c}{V_g}\right)}{\left(1 + (1 + K_{eq,PGM} + K_{eq,PGM}K_{eq,ENO}) \frac{V_c}{V_g}\right)} \quad (\text{Eq. 39})$$

When $[3-PGA]$ was known, $[2-PGA]$ and $[PEP]$ were calculated from Equations 37 and 38, respectively.

d, $2ADP_g \leftrightarrow ATP_g + AMP_g$

The equilibrium equation is

$$\frac{[AMP]_g[ATP]_g}{[ADP]_g^2} = K_{eq,AK} \quad (\text{Eq. 40})$$

Solving the Equations 1, 21, and 40 gives a quadratic equation and the relevant solution is

$$[ATP]_g = \frac{-b_g + \sqrt{b_g^2 - 4a_g c_g}}{2a_g} \quad (\text{Eq. 41})$$

in which

$$a_g = 1 - 4K_{eq} \quad (\text{Eq. 42})$$

TABLE IV
The calculated steady-state glycolytic fluxes under aerobic and anaerobic conditions

Flux	Consumption rate	
	Aerobic	Anaerobic
	$nmol\ min^{-1}(mg\ cell\ protein)^{-1}$	
Glucose	73	71
O ₂	73	0
Pyruvate	-147	-71
Glycerol	0	-71

$$b_g = C_1 - P_g(1 - 4K_{eq,AK}) \quad (\text{Eq. 43})$$

$$c_g = -K_{eq}P_g^2 \quad (\text{Eq. 44})$$

The other solution of the quadratic equation gives negative concentrations of ADP and was not considered. The concentrations of ADP and AMP were calculated from Equations 21 and 1, respectively. To obtain the cytosolic concentrations $[ATP]_c$, $[ADP]_c$, and $[AMP]_c$ P_c was substituted for P_g .

Numerical Methods—The simulations were performed with the program MLAB (Civilized Software, Bethesda). First a time-dependent simulation was performed by integrating Equations 23–32 with a Gear-Adams algorithm, until the system approached a steady state. Usually the initial values of all independent variables were arbitrarily chosen to be 1. Subsequently, the system of nonlinear equations defining the steady state was solved with a Marquardt-Levenberg algorithm, to which the final metabolite concentrations of the time-dependent simulation were given as initial values. An imposed constraint was that all concentrations should be positive, and, if they were involved in a conserved moiety, they should be smaller than the corresponding conserved sum. Finally, starting from the obtained solution a second time integration was performed to test the stability of the steady state. It was examined whether the steady state was unique, by varying the initial metabolite concentrations over a wide range. This never gave a different steady state, but this cannot be considered definite proof of uniqueness.

RESULTS

Fluxes and Concentrations Under Aerobic and Anaerobic Conditions—The first question we addressed was whether the combination of all information on the *in vitro* kinetics of the glycolytic enzymes leads to realistic fluxes and metabolite concentrations. We therefore calculated the steady-state glycolytic fluxes and metabolite concentrations using the model as described above. The rate of glucose consumption hardly changed upon a shift from aerobic to anaerobic conditions (Table IV). This is in agreement with measurements by Visser (38) who observed that the sum of pyruvate and glycerol production was the same under both conditions. Under aerobic conditions glucose was fully converted to pyruvate, while under anaerobic conditions equimolar amounts of pyruvate and glycerol were produced. The predicted cytosolic concentrations of DHAP, PEP, pyruvate, Gly-3-P, and $[ATP]/[ADP]$ differed by less than a factor 2 from the measured cellular concentrations (27, 31) (Table V). The predicted concentrations of 3-PGA and 2-PGA deviated more from the concentrations obtained experimentally. The model-calculated ratios of the concentrations under aerobic and anaerobic conditions corresponded more closely to the experimental ratios. The concentration of Gly-3-P increased by a factor of 4 upon the shift from aerobic to anaerobic conditions, fully in agreement with the measurements (27). For the cytosolic pyruvate concentration and $[ATP]/[ADP]$ ratio under aerobic conditions the correspondence between the model and the experiments was imposed, because the V_{max} of the pyruvate transporter and the equation for ATP utilization were adjusted to fit these concentrations. The $[ATP]/[ADP]$ ratio and the flux under anaerobic conditions, however, were kept free. Only the relation between the two was set by Equation 15.

Interestingly, the calculated $[ATP]/[ADP]$ ratios in the cy-

TABLE V
The steady-state metabolite concentrations under aerobic and anaerobic conditions

The values shown in brackets are the concentrations measured by Visser and Opperdoes (27). To express the latter concentrations in mM, 1 g of wet weight corresponded to 80 mg of protein and 1 ml of total cellular volume corresponded to 175 mg of total cell protein (29). Pyruvate was measured by Wiemer *et al.* (31). The equations and parameter values are specified under "Materials and Methods." To simulate aerobic conditions V_{GK} was set to zero, while under anaerobic conditions V_{GPO} was set to zero.

Metabolite	Concentration		Ratio, aerobic/ anaerobic
	Aerobic	Anaerobic	
	mM		
Glucose (c/g) ^a	0.056	0.10	
Glc-6-P (g)	0.44	0.44	
Fru-6-P (g)	0.13	0.13	
Fru-1,6-bisphosphate (g)	26	2.3	
DHAP (c/g)	1.6 (2.6)	0.61 (1.1)	2.6 (2.3)
GA-3-P (g)	0.074	0.027	
1,3-BPGA (g)	0.028	0.0097	
3-PGA (c/g)	0.68 (4.8)	0.46 (1.2)	1.5 (4.1)
2-PGA (c)	0.13 (0.59)	0.085 (0.33)	1.5 (1.8)
PEP (c)	0.85 (0.74)	0.57 (0.39)	1.5 (1.9)
pyruvate (c)	21 (21)	1.6	
Gly-3-P (g)	1.1 (2.0)	4.2 (7.9)	0.26 (0.25)
[NADH]/[NAD ⁺] (g)	0.036	0.040	
[ATP]/[ADP] (g)	0.48	0.29	
[ATP]/[ADP] (c)	2.9 (2.9)	1.4 (1.2)	2.1 (2.4)

^a c, cytosolic; g, glycosomal.

TABLE VI
Steady-state Γ/K_{eq} for the reversible glycosomal enzymes that were not assumed to be in equilibrium

These were calculated with the equilibrium constants as they were implicitly used in the kinetic equations. The values given in brackets are the Γ/K_{eq} ratios in cell extracts (27).

Enzyme	Γ/K_{eq}	
	Aerobic	Anaerobic
Glucose transport	$1.1 \cdot 10^{-2}$	$2.1 \cdot 10^{-2}$
ALD	$1.8 \cdot 10^{-1}$ (4.3)	$2.4 \cdot 10^{-1}$
GAPDH	$3.1 \cdot 10^{-1}$ ($8.9 \cdot 10^{-1}$)	$3.2 \cdot 10^{-1}$
PGK	$3.6 \cdot 10^{-3}$ ($1.6 \cdot 10^{-2}$)	$4.2 \cdot 10^{-3}$ ($1.6 \cdot 10^{-3}$)
GDH	$4.4 \cdot 10^{-3}$ (1.0, assumed)	$4.0 \cdot 10^{-2}$ (1.0, assumed)

tosol and the glycosome differed by up to a factor of 6, as a consequence of compartmentation. The modeled displacement from equilibrium of reversible reactions, expressed as Γ/K_{eq} , was compared with measurements in cell extracts (27) (Table VI). These measurements were dominated by the cytosolic concentrations, as the glycosomal volume is only 4.3% of the total cellular volume. The measured $\log \Gamma/K_{eq}$ of GAPDH corresponds fairly well with the value predicted from the model. PGK and ALD were in the model further displaced from equilibrium than they were experimentally. GDH was assumed to work in equilibrium by Visser and Opperdoes (27), but according to the model this enzyme was far displaced from equilibrium. This demonstrates that enzymes that are near equilibrium in the cytosol may work far from equilibrium in the glycosome.

Glycerol Titration Under Anaerobic and Aerobic Conditions—Under anaerobic conditions Gly-3-P is converted to glycerol by GK (2). As the $\Delta G_0'$ of this reaction is strongly positive, glycerol effectively inhibits glycolysis at low concentrations (50% inhibition at 0.8 mM) (39). In the model, glycolysis was also inhibited by glycerol (Fig. 2), but 0.1 mM of glycerol reduced the glucose consumption already by 96.1%. Increasing the forward and reverse V_{max} of GK, *i.e.* the amount of the enzyme, did not increase the resistance to glycerol (result not shown). The model concentration of Gly-3-P in the presence of 0.1 mM glycerol was 5.1 mM which is equal to the K_M of GK for

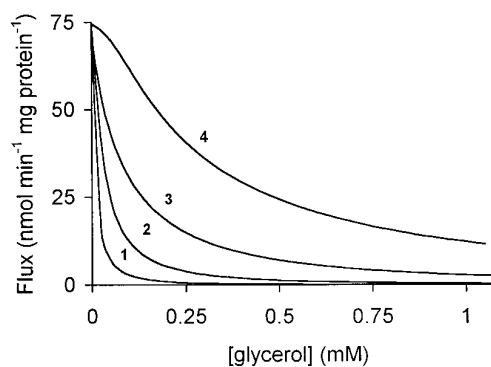


Fig. 2. The steady-state glucose consumption rate under anaerobic conditions as a function of the glycerol concentration as modeled for various combinations of C_4 and the K_M of GK for glycerol. 1, $C_4 = 120$ mM and $K_{M, \text{glycerol}} = 0.12$ mM; 2, $C_4 = 360$ mM and $K_{M, \text{glycerol}} = 0.12$ mM; 3, $C_4 = 120$ mM and $K_{M, \text{glycerol}} = 1.2$ mM; 4, $C_4 = 360$ mM and $K_{M, \text{glycerol}} = 1.2$ mM. All other equations and parameters can be found under "Materials and Methods."

this metabolite. Gly-3-P is involved in one conserved moiety and, as it equilibrates across the glycosomal membrane, it is weighted by a factor 23.3. Thus a large decrease of other concentrations in this sum is required to compensate for an increase of Gly-3-P (Equation 5). It was conjectured that C_4 became a limiting factor under anaerobic conditions. Indeed, an increase of C_4 , from 120 to 360 mM, substantially increased the flux in the presence of glycerol (Fig. 2) with a concomitant increase of [Gly-3-P] (not shown). A 10-fold increase of the K_M of GK for glycerol, and thus the equilibrium constant of GK, further improved the glycerol resistance. A combination of both ($C_4 = 360$ mM and $K_{M, \text{glycerol}}^{\text{GK}} = 1.2$ mM) gave the maximum glycerol resistance. At a C_4 of 360 mM, however, under aerobic conditions the glycosomal concentration of fructose 1,6-bisphosphate (Fru-1,6-BP) increased to 136 mM. The concomitant increase of the osmotic pressure in the glycosomes might then lead to swelling or even bursting of the organelles. Obviously, simply increasing C_4 is not a realistic option.

Under aerobic conditions glycerol can be used as a substrate. This was simulated by including both GK and GPO in the model and by substituting glycerol for glucose. The modeled rate of pyruvate production from 10 mM of glycerol was 80% of the rate from 10 mM of glucose, while experimentally only 50–60% was found (39, 40). This discrepancy disappeared when the V_{max} of GPO was decreased by 40% from 368 to 220 nmol Gly-3-P min^{-1} (mg protein^{-1}). Then the rate of pyruvate production at 10 mM of glucose was 134 nmol min^{-1} (mg protein^{-1}) compared with 79 nmol min^{-1} (mg protein^{-1}) (59%) at 10 mM of glycerol. Actually a GPO activity as low as 171 nmol Glc-3-P min^{-1} (mg protein^{-1}) has also been reported for bloodstream form *T. brucei* at 25 °C (41).

Variation of the Extracellular Glucose Concentration: the Model as Interpreter—Using the silicone oil centrifugation technique Ter Kuile *et al.* (23) demonstrated that the intracellular glucose concentration $[\text{Glc}]_i$ remained very low when the extracellular glucose concentration $[\text{Glc}]_o$ was kept below 5 mM. Above a $[\text{Glc}]_o$ of 5 mM a drastic increase of $[\text{Glc}]_i$ was observed. The model reproduced this (Fig. 3, full lines), although the calculated $[\text{Glc}]_i$ remained lower than the measured $[\text{Glc}]_i$. The difference between model and experiment became most pronounced at the higher concentrations; at 10 mM of $[\text{Glc}]_o$ the measured $[\text{Glc}]_i$ was 1.9 mM, whereas the calculated $[\text{Glc}]_i$ was only 0.3. This difference was due to the fact that the used assay does not distinguish between glucose and Glc-6-P (23). The Glc-6-P concentration averaged over the whole cell was 1.6 mM (27). This concentration should not be confused with the calculated glycosomal concentration. Subtraction of Glc-6-P gives a

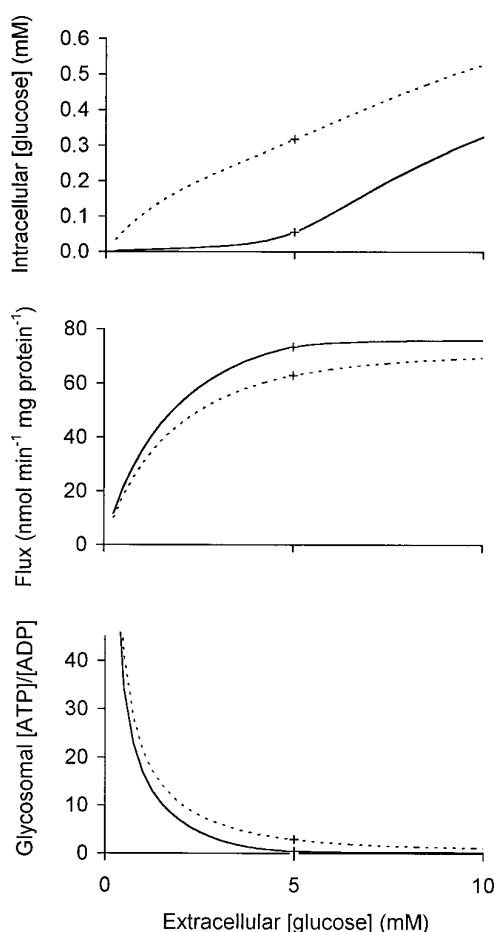


FIG. 3. The intracellular concentration of glucose, the glycolytic flux, and the glycosomal [ATP]/[ADP] ratio as a function of the extracellular concentration of glucose under aerobic conditions. For the glycolytic flux the steady-state rate of glucose transport was taken. The full lines were calculated with the parameter set as described under "Materials and Methods." Only above 5 mM glucose extracellularly the model showed an accumulation of intracellular glucose. The biphasic increase of the intracellular glucose concentration was lost when the K_M of HK for glucose was changed to 2 mM (dashed lines).

[Glc]_i of 0.3 mM, which fits the value calculated by the model.

A mathematical model may serve to test the feasibility of proposed mechanisms. Along this line it was investigated whether the biphasic increase of intracellular glucose could be related to the fact that glucose transport has a 20-fold higher K_M for intracellular glucose than HK. Indeed, when the model K_M of HK was increased from 0.1 to 2 mM (Fig. 3, dashed lines) or when the K_M of the glucose transporter was decreased from 2 to 0.1 mM (results not shown), the biphasic character of the curve disappeared.

To understand this phenomenon, let us first examine the case in which glucose uptake has a K_M of 2 mM and HK has a K_M of 0.1 mM for intracellular glucose. An increasing extracellular glucose concentration should cause an increased influx of glucose. As the K_M of HK is relatively low, a small increase of [Glc]_i should suffice to increase the flux through HK so as to cope with the increased influx. In the limit to an extracellular glucose concentration of zero, the derivative of $v_{\text{glucose transport}}$ to [Glc]_i is zero, which means that initially the influx rate is insensitive to [Glc]_i. This is what happens during the first phase when at low [Glc]_o the [Glc]_i remains low. At increasing [Glc]_o the influx increases further, until [Glc]_i saturates HK, so that a further increase of [Glc]_i does not lead to a higher rate of phosphorylation. Consequently, [Glc]_i starts accumulating un-

til it inhibits the influx rate to the extent that a steady state is attained. This is what happens in the second phase where [Glc]_i is accumulating. As the K_M values are so different there is only a very small range of glucose concentrations at which both glucose transport and HK are sensitive to [Glc]_i and, therefore, the switch between the two phases is very sudden.

If the K_M of HK for [Glc]_i were increased to 2 mM, a higher [Glc]_i should be required to stimulate HK, and this should already lead to a deceleration of glucose transport. In this case there should exist a broad range of [Glc]_i values at which both the transporter and HK are sensitive to [Glc]_i, so that no sudden switch should be expected. Consistently, the calculated [Glc]_i was higher and the flux lower under these conditions.

Under both conditions, *i.e.* low and high K_M of HK, the glycosomal [ATP]/[ADP] ratio decreased drastically with increasing flux. This was required for the PGK further downstream to be able to cope with the increased flux. A side effect is, however, that a decreasing [ATP]/[ADP] ratio inhibits the flux through HK. Thus, the increasing [Glc]_i serves partly to compensate for the decreased [ATP]/[ADP] ratio. If one treats HK and the further metabolism of glucose as one block (42, 43), it has an even higher affinity for glucose than HK on its own. This should make the biphasic shape of the [Glc]_i curve more pronounced, and, furthermore, it explains why the switch occurs when [Glc]_i is still below the K_M of hexokinase for [Glc]_i.

Sensitivity Analysis—One cannot expect all kinetic constants taken from the literature to be precisely correct. Therefore, we examined whether the results of our calculations depended strongly on the parameter values. All parameter values were varied independently by plus and minus 50% (results not shown). The system always evolved to a new steady state. Three types of responses were observed. Changes of some parameters, such as the equilibrium constant of AK, hardly caused any changes. In other cases only local effects were seen, *e.g.* variation of the K_M of PGK for ATP led to a small change of the glycosomal [ATP]/[ADP] ratio. Some parameter changes led to global changes, mostly transmitted via the coenzymes. For instance an increase of the K_M of GAPDH for GA-3-P led to a decrease of the flux, the [ATP]/[ADP] ratio in both compartments, the [NADH]/[NAD⁺] ratio, and the concentration of 1,3-bisphosphoglycerate (1,3-BPGA), and, furthermore, to an increase of intracellular glucose [Glc]_i and triose phosphate. However, the effects on the flux were rather small. The flux varied between 91 and 104% of the unmodulated flux when all possible parameter changes were taken into account. Only if the amounts of enzymes were decreased (*i.e.* the V_{max}), larger changes were observed but always below 50%.

DISCUSSION

We constructed and tested an integral kinetic model that describes the steady-state behavior of glycolysis in the bloodstream form of *T. brucei* quantitatively. The model operates at the metabolic level (44). Because transcription and translation have not been included, the model may be limited to cells that do not grow or alter gene expression. Such conditions occur, for instance, in isolated cells in the absence of any nitrogen source, but in the presence of glucose. The model contains experimentally obtained kinetic expressions for most glycolytic enzymes in *T. brucei*. Because no information is available on the kinetics of transport of metabolites across the glycosomal membrane, the transport of glucose across the cytosolic and the glycosomal membrane was lumped, and the other transport steps across the latter membrane were assumed to be at equilibrium. Another limitation was the fact that the enzyme kinetics had been measured at 25 °C, while physiological studies had been performed at 37 °C. For this reason, relative changes of the flux rather than absolute fluxes were considered when the model

was compared with experimental results. To the extent that the K_M values of the enzymes depend on the temperature and to the extent that the V_{\max} values of different enzymes exhibit different temperature dependences, one should expect the steady-state metabolite concentrations to depend on the temperature.

As all parameter values included in the model are based on measurements there may be experimental errors in them. Therefore, it was tested how the model reacted to variations of its parameters. Both local and global effects were observed. This was to be expected, because any realistic model should represent the flexibility of the living cell. However, the effects were relatively small, and particularly, none of the parameter changes affected the stability of the steady state. Therefore, we trust that minor adjustments of these parameters will not overturn our conclusions.

The model constructed in this paper was virtually completely based on *in vitro* determined enzyme kinetic data. It was not based on a data fit. In view of this, the model predictions correspond remarkably well to experimental data. The relative changes of the flux corresponded exactly, when aerobic and anaerobic conditions were compared. Also most metabolite concentrations deviated less than a factor 2 from the measured concentrations as far as these were available. The available concentrations have been measured in cell extracts, so if the glycosomal concentration is neglected because of the small relative volume of the glycosomes, they represent the cytosolic concentrations. As they were expressed on the basis of wet weight, which is not very accurate, the ratios of concentrations under aerobic and anaerobic conditions should be much more accurate than the absolute concentrations. Indeed these ratios corresponded even better between model and experiment. Only the ratio of the 3-PGA concentrations did not correspond (1.5 calculated *versus* 4.1 mM measured). This may indicate that the assumption of equilibrium of 3-PGA transport, PGM, and ENO is an oversimplification.

The intracellular glucose concentration as a function of the extracellular glucose concentration is an interesting example, where the model not only mimics the experiments quantitatively but also explains them. It was demonstrated that the biphasic relation between the intracellular and extracellular glucose concentrations was caused by the large difference of the K_M values of glucose transport and HK for intracellular glucose. As glucose is transported via facilitated diffusion, *i.e.* down a concentration gradient, it is not unlikely that the second transport step has an intermediate affinity. It remains to be investigated how this will affect the intracellular glucose concentration in the model.

The main discrepancy between the model and the experiments, at least quantitatively, concerned the anaerobic glycerol titration. Both in real cells and in the model glycerol fully inhibited the glycolytic flux under anaerobic conditions, the difference being that much less glycerol was needed in the model. The glycerol tolerance in the model could be improved by shifting the equilibrium of GK more toward glycerol production and, more notably, by increasing the conserved sum C_4 . A shift of the GK equilibrium is not realistic as the enzyme kinetics have been determined in the presence of $[Mg^{2+}]$, so that the equilibrium was maximally shifted in the direction of glycerol (6). An increase of C_4 under aerobic conditions led to an enormous accumulation of Fru-1,6-BP. The cause of this is that Gly-3-P contributes enormously to C_4 , because not only the glycosomal but also the cytosolic fraction is included. Thus, an increase of the Gly-3-P concentration required to drive the GK reaction leads to a relatively large decrease of other metabolite concentrations and vice versa. This restriction may be relieved

when the transport of Gly-3-P is coupled to the transport of DHAP. In that case the conservation equation of organic phosphate groups that are not exchanged with inorganic phosphate (Equation 5), is replaced by two equations:

$$[\text{Gly-3-P}]_g + [\text{DHAP}]_g + [\text{Glc-6-P}]_g + [\text{Fru-6-P}]_g + 2[\text{Fru-1,6-BP}]_g + [\text{GA-3-P}]_g + [1,3\text{BPGA}]_g + 2[\text{ATP}]_g + [\text{ADP}]_g = C_4 \quad (\text{Eq. 45})$$

and

$$[\text{Gly-3-P}]_c + [\text{DHAP}]_c = C_5 \quad (\text{Eq. 46})$$

Then a change of the Gly-3-P concentration in the glycosome should have only small effects on the other metabolite concentrations. This should also exclude the possibility of a high osmotic pressure in the glycosomes in case of a drop of Gly-3-P and DHAP.

Glycosomal concentrations of Glc-6-P (4.4 mM), Fru-6-P (2.4 mM), Fru-1,6-BP (1.9 mM), DHAP (7.1 mM), GA-3-P (0.47 mM), and 1,3-BPGA (0.77 mM) have been estimated (45) on the basis of pulse-chase experiments (24). Except for [Fru-1,6-BP], these concentrations are 1 order of magnitude higher than the concentrations predicted by the model. One reason for the discrepancy may be the fact that the model neglects sequestration of metabolites by the enzymes, which may contribute substantially to the total metabolite concentrations due to the high intraglycosomal enzyme concentrations (46). However, the concentrations given by Misset and Opperdoes (45) were estimations. According to the pulse-chase experiments (24) 20–30% of hexose monophosphate (Glc-6-P plus Fru-6-P) and Fru-1,6-BP were labeled in the first fast phase (15 s) and the remaining 70 to 80% in the second slow phase (500 s and longer). The time constant of labeling is related to the size of a metabolite pool divided by the flux through this pool (47). Biphasic labeling kinetics imply that only part of a metabolite pool lies on the mainstream of metabolism but do not specify its location. The quickly labeled fraction was interpreted to be the glycosomal fraction and the slowly labeled fraction to be the cytosolic fraction (24). The phosphoglycerates and PEP, however, were also labeled in two phases. The authors themselves suggested that PGM, ENO, and PYK might be attached to the glycosomes, but there is no direct evidence for this. Even if the concentrations of the hexose monophosphates and Fru-1,6-BP were correct, the estimated concentrations of DHAP, GA-3-P, and 1,3-BPGA should be considered with care. They were based on the total cellular concentrations, and the assumption that also for these metabolites the glycosomal fraction was 20–30% of the total amount. We have shown, however, that at the measured enzyme activities ALD, GAPDH, PGK, and GDH must work further from equilibrium in the glycosome than in the cytosol to support the high glycolytic flux. Therefore, one should perhaps refrain from extrapolating average cellular concentrations to glycosomal concentrations. Obviously it becomes important now to measure all glycosomal metabolite concentrations unambiguously.

In conclusion, we may say that our model shows that most of the available experimental data are consistent with each other, *i.e.* fluxes and concentrations are largely predicted by the known kinetic properties of the enzymes. To optimize the model, extra data on the transport of metabolites across the glycosomal membrane and on the intraglycosomal metabolite concentrations are required. In the light of the good correspondence between the model and the experiments, we expect the model to serve as a valuable heuristic tool. In particular we plan to use it to predict how the glycolytic flux depends quantitatively on the different enzyme activities. This then may prove to be very helpful in the search for new drugs against sleeping sickness.

Acknowledgments—We thank Drs. M. Callens, D. Kuntz, O. Bos, and A.-M. Loiseau for the sharing of unpublished results and B. Teusink, M. C. Walsh, and K. van Dam for careful reading of the manuscript and fruitful discussions.

REFERENCES

1. Opperdoes, F. R., and Borst, P. (1977) *FEBS Lett.* **80**, 360–364
2. Opperdoes, F. R. (1987) *Annu. Rev. Microbiol.* **41**, 127–151
3. Michels, P. A. M., and Hannaert, V. (1994) *J. Bioenerg. Biomembr.* **26**, 213–219
4. Hannaert, V., and Michels, P. A. M. (1994) *J. Bioenerg. Biomembr.* **26**, 205–212
5. Bakker, B. M., Westerhoff, H. V., and Michels, P. A. M. (1995) *J. Bioenerg. Biomembr.* **27**, 513–525
6. Hammond, D. J., and Bowman, I. B. R. (1980) *Mol. Biochem. Parasitol.* **2**, 77–91
7. Hammond, D. J., Aman, R. A., and Wang, C. C. (1985) *J. Biol. Chem.* **260**, 15646–15654
8. Nwagwu, M., and Opperdoes, F. R. (1982) *Acta Trop.* **39**, 61–72
9. Cronin, C. N., and Tipton, K. F. (1987) *Biochem. J.* **245**, 13–18
10. Cronin, C. N., and Tipton, K. F. (1985) *Biochem. J.* **227**, 113–124
11. Van Schaftingen, E., Opperdoes, F. R., and Hers, H.-G. (1985) *Eur. J. Biochem.* **153**, 403–406
12. Callens, M., Kuntz, D. A., and Opperdoes, F. R. (1991) *Mol. Biochem. Parasitol.* **47**, 19–30
13. Callens, M., and Opperdoes, F. R. (1992) *Mol. Biochem. Parasitol.* **50**, 235–244
14. Van Schaftingen, E., Opperdoes, F. R., and Hers, H.-G. (1987) *Eur. J. Biochem.* **166**, 653–661
15. Michels, P. A. M. (1988) *Biol. Cell* **64**, 157–164
16. Rapoport, T. A., Heinrich, R., Jacobasch, G., and Rapoport, S. (1974) *Eur. J. Biochem.* **42**, 107–120
17. Fell, D. A. (1992) *Biochem. J.* **286**, 313–330
18. Westerhoff, H. V., and Van Dam, K. (1987) *Thermodynamics and Control of Biological Free-energy Transduction*, Elsevier Science Publishers B.V., Amsterdam
19. Garfinkel, D., Frenkel, R. A., and Garfinkel, L. (1968) *Comput. Biomed. Res.* **2**, 68–91
20. Galazzo, J. L., and Bailey, J. E. (1990) *Enzyme Microb. Technol.* **12**, 162–172
21. Cortassa, S., and Aon, M. A. (1994) *Enzyme Microb. Technol.* **16**, 761–770
22. Kashiwaya, Y., Sato, K., Tsuchiya, N., Thomas, S., Fell, D. A., Veech, R. L., and Passonneau, J. V. (1994) *J. Biol. Chem.* **269**, 25502–25514
23. Ter Kuile, B. H., and Opperdoes, F. R. (1991) *J. Biol. Chem.* **266**, 857–862
24. Visser, N., Opperdoes, F. R., and Borst, P. (1981) *Eur. J. Biochem.* **118**, 521–526
25. Marchand, M., Kooystra, U., Wierenga, R. K., Lambeir, A.-M., Van Beeumen, J., Opperdoes, F. R., and Michels, P. A. M. (1989) *Eur. J. Biochem.* **184**, 455–464
26. Lambeir, A.-M., Opperdoes, F. R., and Wierenga, R. K. (1987) *Eur. J. Biochem.* **168**, 69–74
27. Visser, N., and Opperdoes, F. R. (1980) *Eur. J. Biochem.* **103**, 623–632
28. Sauro, H. M., and Fell, D. A. (1991) *Math. Comput. Modell.* **15**, 15–28
29. Opperdoes, F. R., Baudhuin, P., Coppens, I., De Roe, C., Edwards, S. W., Weijers, P. J., and Misset, O. (1984) *J. Cell Biol.* **98**, 1178–1184
30. Wiemer, E. A. C., Ter Kuile, B. H., Michels, P. A. M., and Opperdoes, F. R. (1992) *Biochem. Biophys. Res. Commun.* **184**, 1028–1034
31. Wiemer, A. C., Michels, P. A. M., and Opperdoes, F. R. (1995) *Biochem. J.* **312**, 479–484
32. Stein, W. D. (1986) *Transport and Diffusion Across Cell Membranes*, pp. 237–257, Academic Press, London
33. Eienthal, R., Game, S., and Holman, G. D. (1989) *Biochim. Biophys. Acta* **985**, 81–89
34. Segel, H. I. (1975) *Enzyme Kinetics: Behavior and Analysis of Rapid Equilibrium and Steady-state Enzyme Systems*, pp. 544–560, Wiley Interscience, New York
35. Callens, M., Kuntz, D. A., and Opperdoes, F. R. (1991) *Mol. Biochem. Parasitol.* **47**, 1–10
36. Nolan, D. P., and Voorheis, H. P. (1991) *Eur. J. Biochem.* **202**, 411–420
37. Nolan, D. P., and Voorheis, H. P. (1992) *Eur. J. Biochem.* **209**, 207–216
38. Visser, N. (1981) *Carbohydrate Metabolism in Erythrocytes and Trypanosomes*. Ph.D. thesis, University of Amsterdam
39. Fairlamb, A. H., Opperdoes, F. R., and Borst, P. (1977) *Nature* **265**, 270–271
40. Kiara, J. K., and Njogu, M. R. (1994) *Biotechnol. Appl. Biochem.* **20**, 347–356
41. Opperdoes, F. R., Borst, P., and Spits, H. (1977) *Eur. J. Biochem.* **76**, 21–28
42. Schuster, S., Kahn, D., and Westerhoff, H. V. (1993) *Biophys. Chem.* **48**, 1–17
43. Rohwer, J. M., Schuster, S., and Westerhoff, H. V. (1996) *J. Theor. Biol.* **179**, 213–228
44. Westerhoff, H. V., Koster, J. G., Van Workum, J. G., and Rudd, K. E. (1990) in *Control of Metabolic Processes* (Cornish-Bowden, A. and Cardenas, M. L., eds), 399–412, Plenum Publishing Corp., New York
45. Misset, O., and Opperdoes, F. R. (1984) *Eur. J. Biochem.* **144**, 475–483
46. Misset, O., Bos, O. J. M., and Opperdoes, F. R. (1986) *Eur. J. Biochem.* **157**, 441–453
47. Easterby, J. S. (1981) *Biochem. J.* **199**, 155–161
48. Lambeir, A.-M., Loiseau, A. M., Kuntz, D. A., Vellieux, F. M., Michels, P. A. M., and Opperdoes, F. R. (1991) *Eur. J. Biochem.* **198**, 429–435
49. Misset, O., and Opperdoes, F. R. (1987) *Eur. J. Biochem.* **162**, 493–500
50. Fairlamb, A. H., and Bowman, I. B. R. (1977) *Exp. Parasitol.* **43**, 353–361
51. Bergmeyer, H. U. (1974) in *Methods of Enzymatic Analysis* (Bergmeyer, H. V., ed) 2 Ed., Vol. 1, Academic Press, New York